Study of Corona Configurations under DC Conditions and Recommendations for an Identification Test Plan

Abdul Madhar, Saliha; Mraz, Petr; Mor, Armando Rodrigo; Ross, Robert

DOI
10.1016/j.ijepes.2020.105820

Publication date
2020

Document Version
Final published version

Published in
International Journal of Electrical Power & Energy Systems

Citation (APA)
Abdul Madhar, S., Mraz, P., Mor, A. R., & Ross, R. (2020). Study of Corona Configurations under DC Conditions and Recommendations for an Identification Test Plan. *International Journal of Electrical Power & Energy Systems*, *118*, 1-10. Article 105820. https://doi.org/10.1016/j.ijepes.2020.105820

Electrical Power and Energy Systems 118 (2020) 105820

Contents lists available at ScienceDirect

Electrical Power and Energy Systems

journal homepage: www.elsevier.com/locate/ijepes

Study of Corona Configurations under DC Conditions and Recommendations for an Identification Test Plan

Saliha Abdul Madhar[a,b,*], Petr Mráz[b], Armando Rodrigo Mor[a], Robert Ross[a]

[a] Delft University of Technology, Mekelweg 4, 2628 CD Delft, the Netherlands
[b] Haefely AG, Birsstrasse 300, 4052 Basel, Switzerland

ARTICLE INFO

Keywords:
Corona
Partial Discharge (PD)
HVDC
Pattern recognition
Pulse Sequence Analysis (PSA)

ABSTRACT

Corona is one of the most common forms of partial discharge (PD) occurring in high voltage (HV) energy systems. The corona mechanism in air is not exclusive to the field of energy applications but has also been widely studied by physicists to theorize mechanisms of charge transfer during the different phases of gas discharge. The phases of the discharge and its corresponding behavior with alternating voltage (AC) are well established and represented through various discharge trends, patterns and stages. This not only makes the identification of the PD defect possible but also helps evaluate the risk. This paper investigates corona configurations under DC stress in an attempt to create a similar outline of the defect as exists under AC. The defect is studied in terms of the pulse sequence information. The measurement system requirements are kept within a realistic realm to preserve applicability to industrial measurements. Finally, it makes selective recommendations for the effective identification of the discharge condition under DC stress.

1. Introduction

Corona is commonly referred to the discharges coming from sharp points at high voltage (HV) in air or other gaseous medium. It is caused by the ionization of the gas due to the excessive electric field stress and this mechanism is described by the nature of the dielectric and the availability of charge carriers. Several pointers exist for corona measurement under AC voltage, such as, the inception of corona on the negative half-cycle before the positive half-cycle, the concentration of the Trichel pulses over the peak of the sine wave, indication of increased risk of flashover after the inception of positive corona (positive streamer) among several others [1]. However, stable and comprehensive indicators of this nature are non-existent when it comes to corona measurement under DC conditions.

A needle-plate corona arrangement is studied by this research in four different configurations based on the position of the needle and polarity of the DC voltage. The several minute differences in each of the four configurations permit the identification of the defect in its various forms. The paper makes recommendations towards an 'Identification Test Plan' to detect are recognize the configuration of corona coming from the device under test.

2. Background

The principal difference between the measurement of AC and DC partial discharges (PD) remains in their evaluation, while the state-of-the-art measuring systems used in both cases remain alike. In case of AC-PD measurements, for each defect there is a unique variation of discharge magnitude over the AC voltage cycle referred to as the phase resolved PD (PRPD) pattern. And considering that discharge inception is defined by one pulse/cycle, the evaluation of the charge value (Q_{iec}) is less dependent of the repetition rate. A miscalculation of the pulse count by the PD evaluation system does not affect the outcomes of the test itself. However, in case of PD measurements under DC voltages, it becomes important to accurately count the number of discharges in a given time period. This means that any outliners/interference, or miscalculation of the pulse count due to duplicate recognition or other means would negatively impact the outcomes of the test as described in [2].

At this moment, it is necessary to highlight an interesting view-point for the DC-PD evaluation, which is to distinguish partial discharges based on the source of the discharge. If one considers the discharges coming from a real geometrical/physical defect, the repetition rate of such PD should be proportional to the time constant of the defect arrangement. In reality, this may be tedious to deduce due to the complex configuration of the defect within the dielectric of the electrical

* Corresponding author.
E-mail address: S.AbdulMadhar@tudelft.nl (S. Abdul Madhar).

https://doi.org/10.1016/j.ijepes.2020.105820
Received 16 July 2019; Received in revised form 4 December 2019; Accepted 3 January 2020

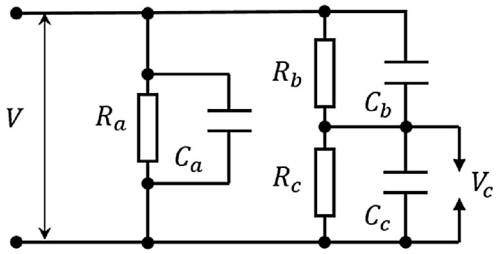

Fig. 1. Classical abc-circuit with leakage resistances to accommodate DC PD.

component. However, strictly for laboratory measurements and specially keeping in mind the measurement of corona in air which this paper discusses, pulses that may occur after the waiting period (time constant) could either be interference pulses from outside or due to effects of space charge, atmospheric influence, or random cosmic radiation.

For example, consider the classical abc-circuit [3] as shown in Fig. 1. Based on the DC model for PD the expression for the voltage over the defect is given by;

$$v_c = \frac{R_c}{R_b + R_c}.\left(1 - e^{-\frac{t}{\tau}}\right).V \tag{1}$$

where τ is the time constant of the defect, R_b *and* R_c are the leakage resistances across the test object and V is the applied DC voltage. This model considers that the field across the defect, in this case a void, is purely due to the electrostatic field of the applied DC voltage.

However, in several cases the electric field due to the accumulated space charges may add to the local electric field stress establishing locally the temporary conditions for discharge inception. These discharges could be referred to as 'pseudo-discharges' since they neither have a stable repetition rate nor a pre-determined range (of PD magnitude). Fig. 2(a) shows a void inside a bounded dielectric with homo-charge formation at the electrode junction. Fig. 2(b) shows the HV electrode of a DC module stationed in air. Due to the electronegative nature of oxygen atoms the electrons attach to them, and in case of higher humidity they attach to water molecules [4], creating a momentary hetero-charge layer as shown. This enhances the electric field between the space charge region and the HV electrode causing erratic corona pulses due to the discharge from the electrode towards the region of the space charge. In order to incorporate this phenomenon, the value of V in Eq. (1) needs to be altered as follows;

$$V = \int_{l=0}^{x} (E_{dc} + E_{sp}(t, r)).\, dl \tag{2}$$

$$E_{sp}(r) = \frac{\rho(s)(r-s)}{|r-s|^3} d^3s \tag{3}$$

where E_{dc} is the electric field due to the applied DC voltage, E_{sp} is the electric field due to the space charge formation, $\rho(s)$ is the charge density with respect to space, s is the unit vector perpendicular to the surface enclosing the charge and r is the point in space where the electric field is calculated. Thus, the volumetric integral of the charge density would equal the divergence of electric field, thereby following Gauss' law/Stroke's theorem.

Therefore, based on Eq. (2), at applied voltage lower than inception, there is still a possibility of PD due to local field enhancement from space charge clouds. However, depending on the charge displacement in the dielectric medium (decay of the space charge) this condition may vary.

Theoretically, once the time constant of the charging circuit is surpassed without the inception of a partial discharge pulse, the voltage can be increased to the next step assuming the availability of an initiating electron. And practically, this is done by measuring the DC voltage immediately across the test object and determining if the voltage settles to the maximum DC value. Especially in the case of corona

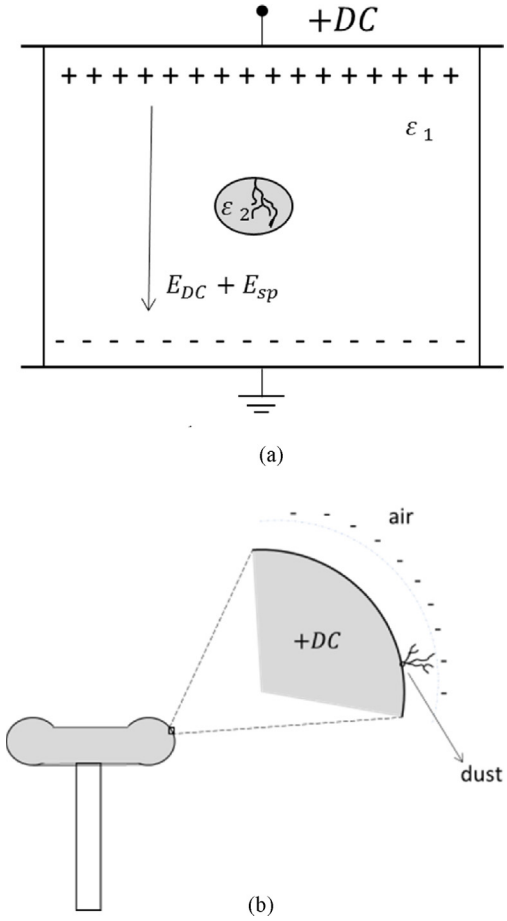

Fig. 2. Pseudo-discharges (a) due to homo-charge formation and (b) hetero-charge formation.

defect in air as this paper investigates, the waiting period should be minimum.

In the following chapters the PD measuring setup, procedure and post-processing tools are described followed by test results of various corona configurations.

3. PD measurement

3.1. Test setup

The test setup is shown in Fig. 3. It comprises of a 100 kV_{rms} AC voltage source that has been tested and certified PD-free, a half-wave rectifier rated for 140 kV_{dc}, a high voltage filter and a $R||C$ voltage divider whose capacitor also serves as the coupling capacitor for PD measurement. The test arrangement in this case is a needle-plate arrangement whose construction is PD free except for the defect fixture (needle).

The distance between the needle and the ground plate is maintained at 25 mm. The measuring impedance in the form of a quadrupole is incorporated in the current measuring loop to decouple the high frequency (HF) PD pulse signal. Additionally, a high frequency current transformer (HFCT) with a measuring band of 20 kHz to 100 MHz is connected under the test arrangement for the possibility of supplementary measurement. The requirements of each of these circuit components and the means to choose them are described in detail in [5].

The tests were repeated several times, using different defect arrangements, different needles (material: stainless steel and brass; and tip radii ~50 to 900 μm), voltage sources and circuit connections to improve reliability of the outcomes and to showcase that the results are

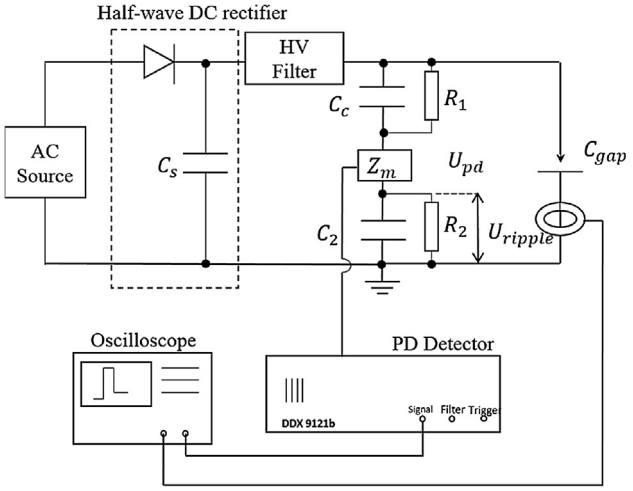

Fig. 3. Schematic of the measuring setup.

not specific towards a certain needle shape or defect configuration. The tests were also performed on different days at different locations at varying temperature and humidity conditions (16–30 °C, up to 60% RH) at atmospheric pressure of 1 atm.

3.2. Measurement procedure

In order to validate the defect arrangement, the arrangement is first tested under AC stress. Based on the AC test, the inception voltage ($U_i$or PDIV) of the Trichel pulses and the positive streamer discharge are noted.

The DC partial discharges are measured by two means. Firstly, through the PD detector (DDX 9121b) which logs data such as the voltage, charge (pC), repetition rate and pulse polarity in real-time. And secondly, using an oscilloscope with a measuring bandwidth (BW) of 250 MHz that is used to stream the raw data coming from the PD detector. As shown in Fig. 3, the 'signal' output channel on the front end of DDX 9121b is used as input to the oscilloscope. This output is independent of the IEC filter settings defined in the detector but can be influenced by the detector's amplifier stage. However, this can be handled manually by setting the amplification level to a fixed value in the detector settings.

The PD measurements are made in free air at atmospheric pressure. The voltage is ramped systematically and the raw data is logged in real-time at each stage. The length of the acquisition depends on the repetition rate (longer acquisition for low repetition rates). The use of an oscilloscope to log the PD raw data, instead of using the measured output of the detector eliminates the errors at the detector stage that might arise due to limited BW and dynamic range that could possibly lead to wrong polarity recognition, double pulse recognition, pulse disappearance and so on. In addition, it is possible to eliminate interference and noise pulses from the acquired pulse stream in the case of raw data acquisition by employing suitable post-processing algorithms for pulse recognition. Before the start of the test (both AC and DC), the setups are calibrated for charge measurement.

In addition to the electrical PD measurement, a corona camera (OFiL Luminar^{HD} Systems) that measures the UV (Ultra Violet) radiation from the discharge site is used parallelly to provide further insight into the discharge phenomenon. It measures highly sensitive UV discharges in the solar blind range of 250–280 nm. The relevant images recorded by the camera are presented in Section 4.

3.3. Post-processing

The acquired raw data is processed in Matlab through a comprehensive set of algorithms that recognize the individual pulses from the data stream and assign them an equivalent charge value based on a calibration factor (quasi-integration) that is pre-programmed. The pulse recognition algorithm is developed based on the equivalent energy threshold of the pulse as presented in [6]. Automated and flexible pulse width identification is used to recognize and count individual pulses. Desired exception handling is employed to ensure reliability of the output.

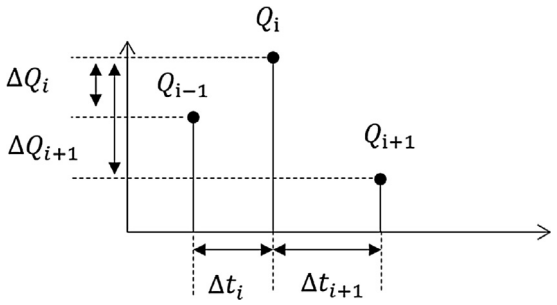

Fig. 4. Graphical representation of the derived quantities from the measured PD raw data.

Several quantities are derived during this phase, such as charge of the pule(Q_i), charge of the successive pulse (Q_{i+1}), difference in charge of two successive pulses (ΔQ_i *and* ΔQ_{i+1}), time of occurrence of pulse (t_i), time of occurrence of successive pulse (t_{i+1}) and difference in time of two successive pulses (Δt_i *and* Δt_{i+1}). These are graphically depicted in Fig. 4.

4. Observations and Results

4.1. Configuration I: DC negative with needle at HV

The first corona configuration investigated is with the needle at negative DC voltage. The detector's filter settings are fixed to the maximum BW of 1 MHz with a center frequency at 600 kHz. The measurement noise floor is 0.03 pC. The progression of the defect configuration with increasing voltage steps is shown in Fig. 5. The corona incepts at −5.75 kV_{dc} (U_i) with a charge magnitude of 120 pC. The discharge stream remains stable in terms of amplitude at the given voltage level. The discharge rate is at 3370 pulses/s. With increasing voltage, the discharge rate increases exponentially while the discharge magnitude drops to about half, ~50 pC. These trends are presented graphically in Fig. 6.

Given the 1 MHz measuring BW of the detector the pulses virtually disappear (virtual pulse-free zone) [1] at 15 kV_{dc} when the pulse

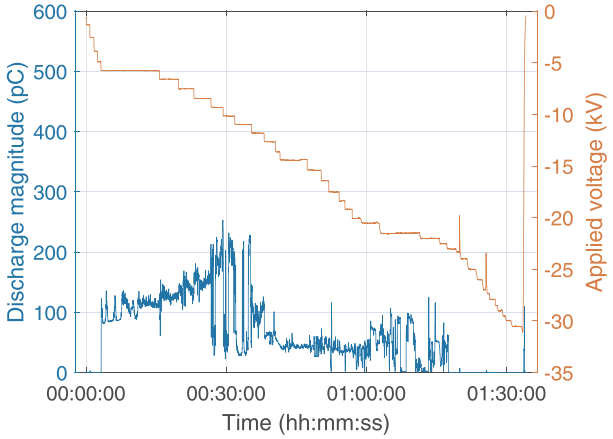

Fig. 5. The progression of the defect (needle at −DC) with increasing voltage (kV_{dc}) as recorded by the PD detector.

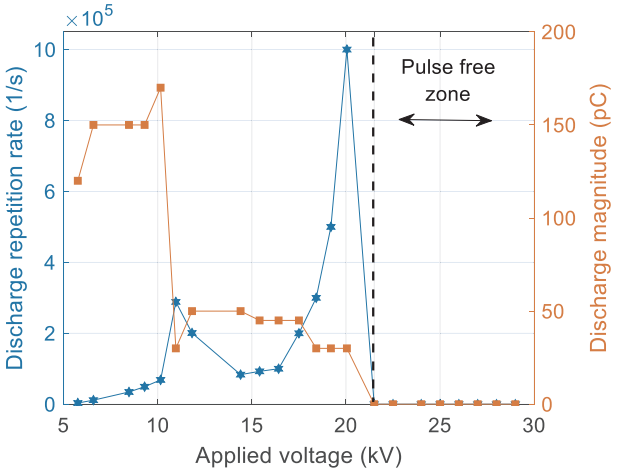

Fig. 6. Discharge repetition rate and magnitude (in pC) as a function of voltage for the needle placed at negative DC voltage.

repetition rate exceeds 1 pulse/μs. However, at this stage, it still remains possible to measure the pulses using the oscilloscope and the HFCT. Close to 20 kV_{dc}, the pulses completely disappear from the electrical domain as shown in Fig. 6. The last value of repetition rates recorded are 800 k–1 M pulses/s.

The corona camera on the other hand can detect the corona around the needle in the pulse-free zone. The image recorded by the corona camera at 20.5 kV_{dc} is shown in Fig. 7. This pulse-free zone extends from 20.5 kV_{dc} until breakdown at 45 kV_{dc} (not shown in figure).

4.1.1. Discharge physics

The physics of the discharge under this configuration can be explained based on the physics of the 'Trichel pulse' [7]. Fig. 8 pictorially depicts the discharge mechanism around the needle tip. The electronegative needle ionizes the air around it when the electric field stress around the tip exceeds the ionization field of air (~3 kV/mm).

Trichel proposed that the formation of negative charges around the needle tip and its subsequent removal resulted in the repetitive discharges. There are primarily two competing mechanisms of discharge in this case; The electron attachment to the electronegative atoms such as oxygen and the electron detachment through excitation and photoionization [8].

$$N_2 + e^- \rightarrow N_2^+ + 2e^-; \quad \Delta H = 104 \ \text{kJ/mol} \tag{4}$$

$$O_2 + e^- \rightarrow O_2^+ + 2e^-; \quad \Delta H = -125 \ \text{kJ/mol} \tag{5}$$

$$O_2 + N_2 + e^- \rightarrow O_2^- + N_2 \tag{6}$$

$$O_2^- + O_2 \rightarrow 2O_2 + e^- \tag{7}$$

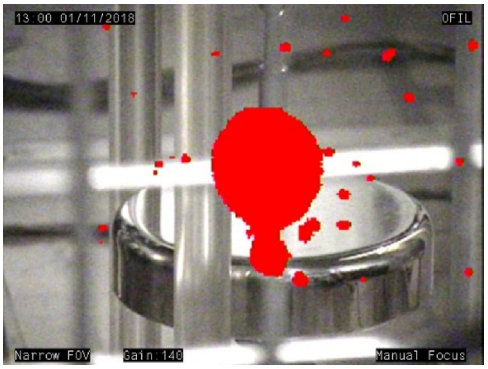

Fig. 7. UV measurement by the corona camera with corona around the needle tip recorded at −20.5 kV_{dc}.

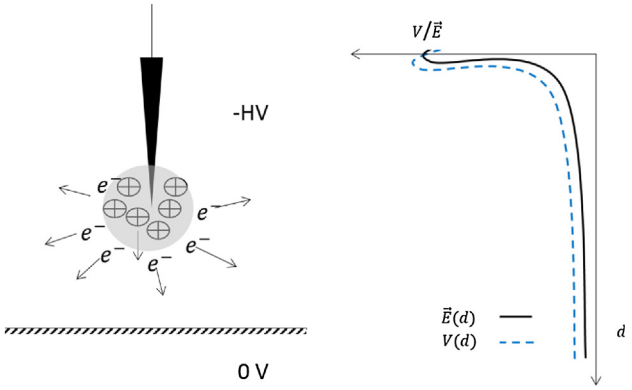

Fig. 8. The mechanism of discharge around the needle tip at −DC voltage and the corresponding voltage and electric field graph across the gap distance, d.

$$O_2 + h\gamma \rightarrow 2O; \quad \Delta H = 498 \ \text{kJ/mol} \tag{8}$$

$$O_2 + O \rightarrow O_3 \tag{9}$$

Though nitrogen (N_2) is the most abundant (78%) gas in atmospheric air, as shown from Eq. (4), the energy for its ionization is higher than for oxygen (O_2). Hence, Eq. (5) is more dominant than Eq. (4) at lower fields. The dissociated electron soon attaches to a neutral oxygen molecule as shown by the 3-body reaction in Eq. (6) creating a negative space charge at a distance away from the needle tip (into the gap). With increasing electric field stress (voltage) the photoionization of oxygen given by Eq. (7) and enhanced electron detachment additionally by Eq. (4) take over [9]. Additionally, the photoionization process strips the oxygen molecule to atomic oxygen, paving the way for the production of ozone, Eqs. (8) and (9). In [10,11] Giao et al. theorize that the increased rate of removal of negative charges and the reduced rate of formation of negative ions due to detachment effect in high fields is responsible for the pulseless region of corona sometimes referred to as 'noisy corona' which is characterized by a DC offset current. In addition, the reduced gas density at the needle vicinity due to elevated temperatures contribute to this phenomenon [12].

The breakdown voltage of this configuration on the other hand is slightly higher since the electrons are dispersed to lower field region and the pre-breakdown requires avalanches to be formed. These avalanches require an electron feedback mechanism that is created by the accelerated positive ions striking the cathode, by the Townsend's mechanism [7].

4.1.2. Discharge patterns

The discharge raw data acquired was utilised to generate several plots based on the quantities mentioned in Section 3.3 including the Pulse Sequence Analysis (PSA) plots that are revered by several researchers [13]. However, the most stable relationship (against increasing voltage level) was obtained for the plot of Charge (Q_{i+1}) vs Time to discharge (Δt_{i+1}) as shown in Fig. 9. This plot represents a unique characteristic of negative corona where the magnitude of discharge is determined by the time elapsed since the previous discharge.

4.2. Configuration II: DC positive with needle at HV

The needle on positive DC voltage incepts at 6.3 kV_{dc} with a discharge magnitude of 0.5–2 pC. The discharge is highly challenging to detect due to the low signal to noise ratio (SNR). Sufficient amplification and filtering stages are required for this measurement. Fig. 10 shows the recorded pulse stream with the high repetition rate which could be mistaken for background noise. This stage of the corona is still possible to be recorded using the corona camera with the discharge concentrated around the needle tip.

Fig. 11 shows the test data log of the charge and voltage over time.

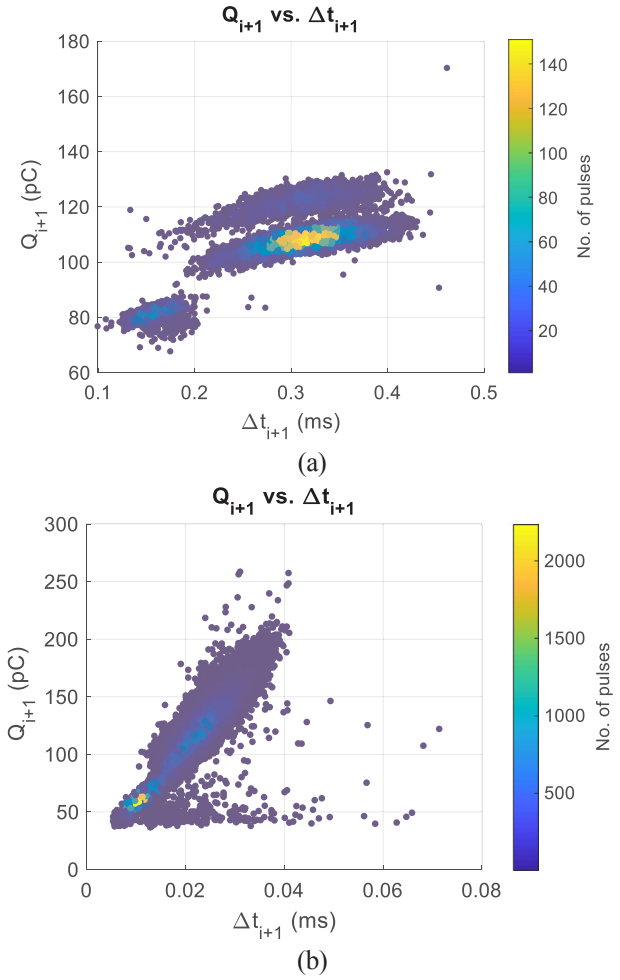

Fig. 9. Discharge pattern of Charge (Q_{i+1}) vs Time to discharge (Δt_{i+1}) (a) at inception voltage of 5.75 kV_{dc} and (b) at 1.6U_i.

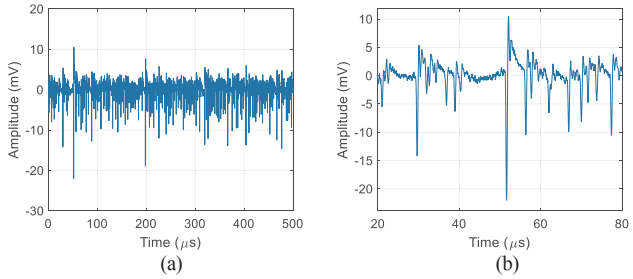

Fig. 10. Discharge pulse stream observed at 6.3 kV_{dc} (a) 0.5 ms acquisition (b) zoomed in to show individual pulses.

It can be noted that at a specific voltage window, 6.4–6.6 kV_{dc} in this case, a stable pulse stream with a discharge magnitude of 400–450 pC incepts. This phenomenon is referred to as 'self-sustaining corona'. It occasionally incepts when the voltage is ramped downwards to this value than by rising the voltage upwards. The 0.5–2 pC (intermittent corona) pulses persist with increasing voltage, getting more repetitive in nature. The UV image captured by the corona-camera increases in intensity and girth. At 18.6 kV_{dc}, larger discharges in excess of a nC begin to incept repetitively indicating a pre-breakdown state.

4.2.1. Discharge physics

Positive corona is described in [14] to occur in three different forms: burst corona, streamer corona and glow corona. The first stage of

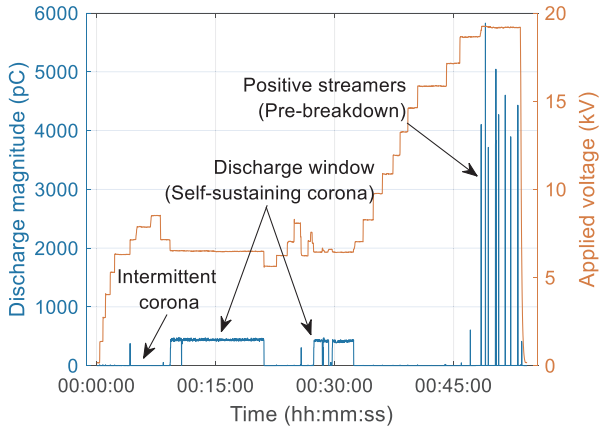

Fig. 11. The progression of the defect (needle at +DC) with increasing voltage (kV_{dc}) as recorded by the PD detector.

corona observed with intermittent pulses has also been reported by Trichel [15]. He describes this phase of corona as being made up with 'imperfectly resolved current impulses of extremely high frequency'. However, he was never able to precisely measure them due to their low energy. This stage of 'intermittent corona' possibly arises from the ionization of the neutral molecules in air, either by impact ionization or photoionization around the needle tip giving rise to a small discharge current as shown by Fig. 12(a). The electric field is maximum at the maxima of the voltage over the needle tip.

The self-sustaining corona that incepts at a specific voltage range is due to a large number of individual current-pulses distributed over the surface of the point in regions of adequate field strength [15]. As depicted in Fig. 12(b) the positive space charge displaced at a distance 'x'

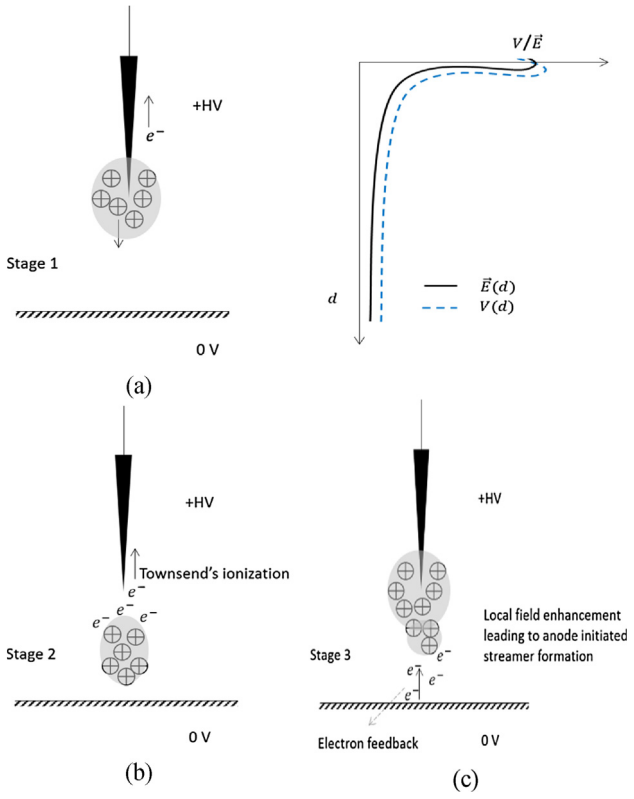

Fig. 12. The mechanism of discharge at the needle tip at +DC voltage (a) intermittent corona at inception and the corresponding voltage and electric field distribution across the gap distance, d (b) self-sustaining corona and (c) streamer corona.

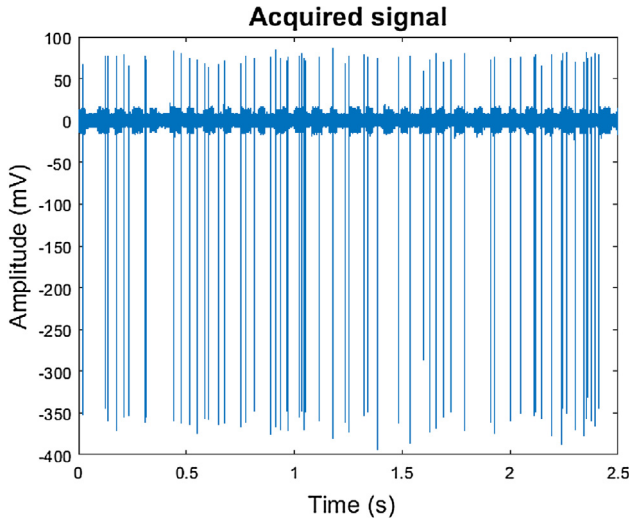

Fig. 13. The discharge pulse sequence at +6.6 kV_{dc}.

from the needle tip with sufficient field strength sustains the Townsend's mechanism of discharge through electron avalanche. Once enough electrons are produced by ionization such that the current is taken care of by the electron avalanche alone, the pulses cease.

At the last stage of the discharge large streamer pulses are observed. These are once again confirmed by Trichel [15]. At higher field strengths the discharge penetrates into the gap and as Trichel describes the appearance of these streamers is relatively sudden. They are believed to be incited by energetic α-rays or properly timed ions. Therefore, the streamers appear to be bursts propagating under 'favourable field conditions.'

4.2.2. Discharge patterns

The intermittent corona stage at inception is challenging to detect correctly and resolve into individual pulses as their occurrence is quite random. They do not create any consistent pattern. The self-sustaining corona pulses with a charge magnitude of 400 pC occur quite repetitively with a stable rate. A 2.5 s pulse sequence is shown in Fig. 13. Fig. 14 with its PSA plot, ΔQ_i *vs* ΔQ_{i+1} shows a vague star pattern, however, the plot of Charge (Q_{i+1}) vs Time to discharge (Δt_{i+1}) shows no relationship indicating that this is unlike the negative corona in configuration I.

4.3. Configuration III: DC negative with needle at ground

Configurations III and IV of the corona arrangements presented in the paper, with the needle placed at ground potential are often not studied, presuming that configurations I and II sufficiently represent III and IV. The mechanism of discharge may be similar; however, several differences exist among them. These are explained in the following

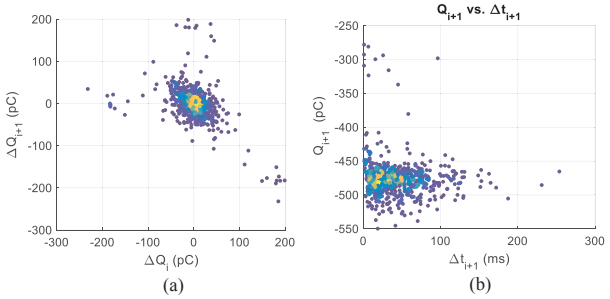

Fig. 14. Discharge patterns of (a) ΔQ_i *vs* ΔQ_{i+1} (PSA) and (b) Charge (Q_{i+1}) vs Time to discharge (Δt_{i+1}) at 6.6 kV_{dc}.

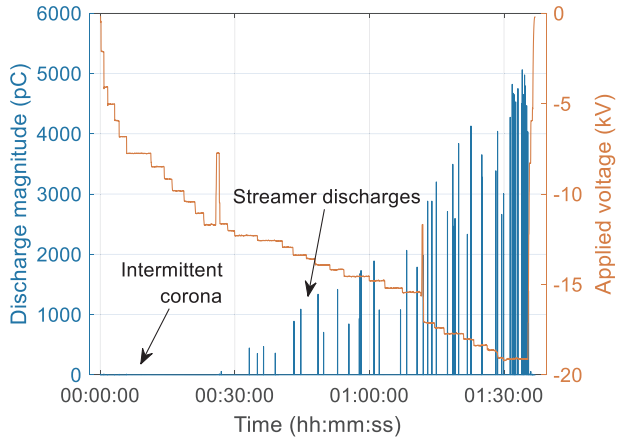

Fig. 15. The progression of the defect (needle at ground; −DC) with increasing voltage (kV_{dc}) as recorded by the PD detector.

sections.

The third corona configuration with the needle placed at ground potential and applying −DC to the plate electrode incepts similar to configuration 2 (needle at + DC) with a 0.5–2 pC stream but at a slightly higher voltage of 7.75 kV_{dc}. The small discharge with intermittent corona persists, while at 11.6 kV_{dc} the first large pulse of amplitude recorded as 60 pC occurs. As can be seen from Fig. 15 with increasing voltage the magnitude of discharge increases almost linearly. At 19.2 kV_{dc} repeated discharges in the order of 5 nC occur indicating a unstable pre-breakdown state. The larger discharges are accompanied with a hissing or whistling sound.

4.3.1. Discharge physics

The physics of the discharge in this configuration is similar to the one described in Section 4.2.1. The needle placed at ground potential is now the anode. The discharge incepts with the intermittent corona creating a small positive charge cloud around the needle. However, the second stage of discharge with the self-sustaining corona is absent in this configuration. This is because of the presence of a cathode in the vicinity of the needle that can provide free electrons via ion-impact on the cathode surface (at HV). Fig. 16 shows the schematic of the discharge mechanism alongside the distribution of voltage and electric field across the gap. These free electrons constantly neutralize the positive space charge. However, at increasing voltages, the streamer corona sets-in similar to the pre-breakdown stage described in Section 4.2.1.

This configuration of corona remains the most dangerous as the streamers incepts at low values of voltage with a large discharge

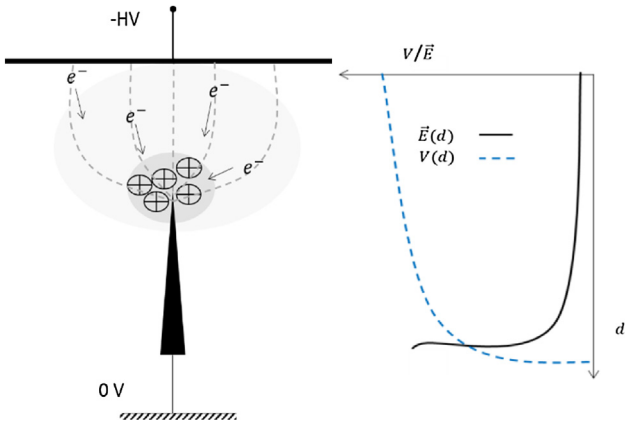

Fig. 16. The mechanism of discharge in configuration III and the corresponding voltage and electric field graph across the gap distance, d.

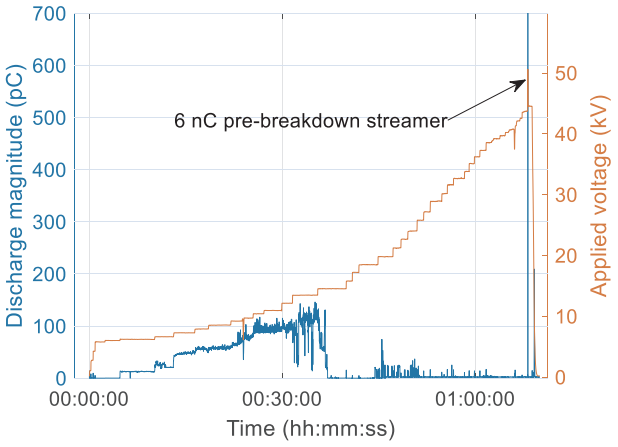

Fig. 17. The progression of the defect (needle at ground; +DC) with increasing voltage (kV_{dc}) as recorded by the PD detector.

magnitude and soon escalates to the unstable-breakdown state if left undetected. Therefore, attention needs to be paid to the ground electrode of DC electrical components, since any damage leading to sharp edges can have severe consequences.

4.4. Configuration IV: DC positive with needle at ground

The final configuration of corona with the needle placed at GND potential and +DC applied to the plate behaves similar to configuration I with needle at −DC. Fig. 17 shows the progression of the corona stages with increasing voltage. The defect incepts at 6.22 kV_{dc} with a discharge magnitude of 12 pC. The discharge repetition rate is 2620/s. With increasing voltage, the discharge magnitude rises from 12 pC at 6.22 kV_{dc} to 110 pC at 13.5 kV_{dc} with a discharge repetition rate of 170,000/s. With further increase in voltage to 14.55 kV_{dc} the repetition rate increases to up to 350,000/s while the discharge magnitude drops to 12–15 pC.

For voltages in excess of 16 kV_{dc}, the pulses disappear from the electrical measurements, denoting a real pulse-free zone as observed in Section 4.1. But until 23 kV_{dc}, the pulse stream with reduced amplitude (12–15 pC) appears and disappears in flashes, denoting a transition phase between Trichel and glow discharge. The pulse-free zone with no discharges persists until a pre-breakdown pulse of 6 nC occurs at 43.6 kV_{dc}. In the pulse-free region (of configuration I and IV) of discharge a small violet glow slightly detached from the needle is observed. The corona camera when used in the pulse-free zone with reduced amplifier gain records a discharge ring around the violet glow as shown in Fig. 18.

Fig. 18. The UV measurement by the corona camera showing the corona ring around the needle tip recorded at 18.5 kV_{dc}.

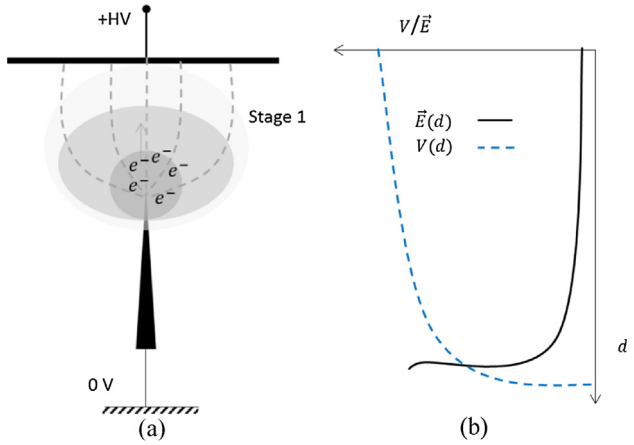

Fig. 19. (a) The mechanism of discharge around the needle tip at GND when +DC applied to the plate and (b) the corresponding voltage and electric field graph across the gap distance (d).

4.4.1. Discharge physics

The discharge physics of this configuration is similar to Section 4.1.1. The differences in inception voltage and discharge magnitude can be explained based on the differences in the electric field strength and voltage distribution of the gap at the same voltage levels. As shown in Fig. 19(b) the electric voltage at the immediate vicinity of the needle tip is slightly reduced than when the needle is directly at HV. This subsequently reduces the resulting electric field stress and hence the reduced magnitude of discharge. Nevertheless, the defect progresses in the same fashion as the needle at −DC.

The violet glow shown in Fig. 18 which appears to be detached from the needle is analogous to the Crookes dark space [7]. The corona ring has also been reported in the past [16] and is due to the field distortion believed to have been caused by the negative space charges in the gap.

4.4.2. Discharge patterns

The discharge patterns obtained in this configuration of corona are well-formed as shown in Fig. 20. However, while comparing the robustness of the obtained diagrams, the discharge pattern of charge (Q_{i+1}) vs time to discharge (Δt_{i+1}) shown in Fig. 20(a) is highly stable and serves as a fingerprint for the identification of the corona/defect. The other patterns are highly sensitive to outliners and disturbances.

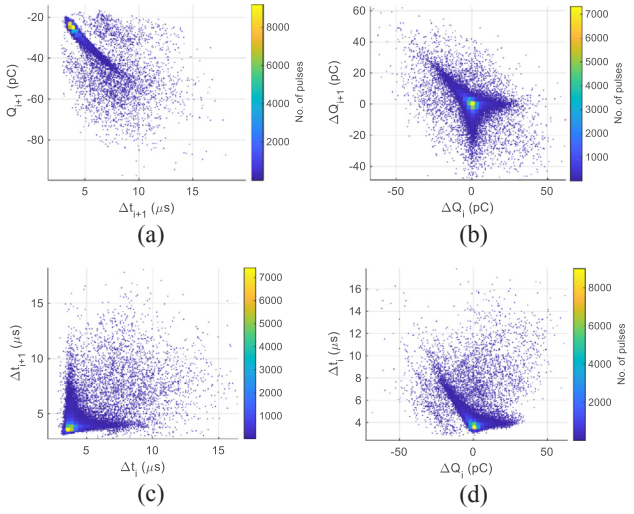

Fig. 20. Discharge patterns of (a) Charge (Q_{i+1}) vs Time to discharge (Δt_{i+1}), (b) ΔQ_i *vs* ΔQ_{i+1} (PSA), (c) Δt_i *vs* Δt_{i+1} (PSA) and (d) ΔQ_i *vs* Δt_i (PSA) at 12.1 kV_{dc}.

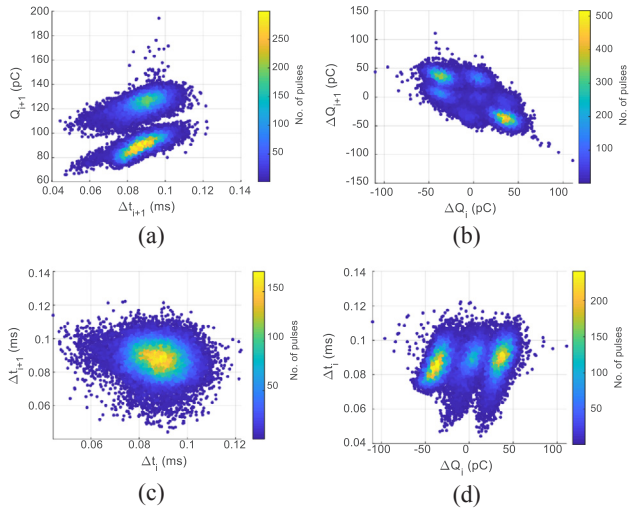

Fig. 21. Discharge patterns of (a) Charge (Q_{i+1}) vs Time to discharge (Δt_{i+1}) (b) ΔQ_i *vs* ΔQ_{i+1} (PSA), (c) Δt_i *vs* Δt_{i+1} (PSA) and (d) ΔQ_i *vs* Δt_i (PSA) at 6.6 kV_{dc} for needle at −DC voltage with 2 corona sources.

For instance, in certain corona configurations a second luminous discharge appears at increased fields/voltages [7]. The discharge alternates between the two spots. Occasionally at still higher voltages, a third spot may appear. This is an inherent characteristic of the corona and depends on the dimensions of the needle tip. The PSA plots in the case of double corona source are completely distorted from the expected form shown in Fig. 20. This is demonstrated through Fig. 21. However, the plot of charge (Q_{i+1}) vs time to discharge (Δt_{i+1}) preserves its unique relationship and even reveals information on the number of discharge sources through the number of clusters.

5. Proposed Identification Test Plan

The possibility of defect identification under DC conditions is still bleak. No stable means of comparison in terms of behavioral pattern has been found for different defects. Nevertheless, corona is by far the only defect that behaves the closest to its AC behavior. The extremely high repetition rates found with corona are not found in any other defect. It also has a unique charge versus voltage (Q vs. V) characteristic for every configuration. Based on these behavioral characteristics of the corona defect it is possible to detect and localise the configuration of corona.

It is possible that at the nominal test voltage, U_{nom}, the defect remains in the pulse-free zone or in the region of intermittent corona (which is difficult to detect). This would lead to the defect going undetected. This is a risky scenario since the pulse-free zone is in reality an active plasma region which corrodes the metallic electrode, leaving behind unwanted residue such as sharp floating particles and poisonous gases. Similarly, if the region of intermittent corona goes undetected, it can lead to streamer discharges due to space charge build-up. Therefore, it is insufficient to do PD measurements on DC components at the value of nominal voltage alone.

Fig. 22 shows a flow chart with a possible test plan that will allow the identification of the corona defect and its respective configuration. The component under test is first tested at its nominal testing voltage over positive polarity (+DC). If PD is measured, an analysis is made on whether the discharge stage has a stable repetition. A stable discharge rate would indicate towards self-sustaining stage of configuration II or negative corona or Trichel of configuration IV. To differentiate between the two configurations, the correlation between the parameters Q_{i+1} *and* Δt_{i+1} is checked. If there exists a trend in the plot of Q_{i+1} *vs* Δt_{i+1} as shown in Fig. 20, it confirms that it is Trichel pulses and hence coming from a protrusion over ground terminal (configuration IV). If there is no correlation in the plot of Q_{i+1} *vs* Δt_{i+1} but the pulses are stable and repetitive, this would indicate the self-sustaining corona stage of configuration II, indicating that the protrusion is close to HV. In case discharge pulses are recorded but they occur randomly, one needs to rule out the possibility that these are streamer discharges of configuration II. Hence, the measurement is repeated at a reduced voltage to look for the self-sustaining or intermittent corona which would confirm that the protrusion is on HV (configuration II). In the event of no pulses being recorded at nominal voltage, one needs to rule out that the component is either under intermittent corona region or under the pulse-free zone. To do this, the measuring sensitivity is increased (by lowering the amplifier gain) to look for pulses close to the noise threshold. The presence of which would confirm that there is a protrusion close to HV (configuration II). However, if absolutely no PD is recorded, the measurement is repeated at reduced voltage until the possibility of pulse-free zone operation is completely ruled out.

Similarly, when the component under test is tested at its nominal testing voltage over negative polarity (−DC), a similar process is followed. Due to the absence of self-sustaining corona stage in configuration III, any discharge with a stable rate would indicate towards the presence of protrusion over HV (configuration I). To rule-out the possibility of operation under pulse-free zone or streamer region, the measurements are repeated with reduced voltage similar to that described for positive DC. The DC components need to be tested at sub-multiples of the nominal voltage to be completely certain of their fitness and quality.

This test plan is a preliminary proposal made based on the information on the corona-defect behavior alone. However, in the future, this can be developed to be component specific (depending on the nature of the dielectric) and inclusive of several defect sources.

6. Discussion

In the 1980s the relevance of partial discharge measurement and diagnostics under DC was mostly applicable only to the field of medical imaging. However, now with increasing HVDC installations such as GIS/GIL, cable links, convertors etc., the method for its design validation and fitness through partial discharge measurement is gaining increasing popularity. This is only expected to rise with the introduction of electric vehicles (EVs) and its related infrastructure. Moreover, given the remarkable success of partial discharge measurements in defect isolation under AC, mounting expectations for a similar prospect under DC conditions is a thriving notion.

Therefore, as a first steps towards characterizing PD defects under DC conditions this contribution rediscovers the physics of the corona progression in detail, in order to recognize minor if not major differences that will enable defect recognition. With the investigation of every additional defect a test plan similar to the one discussed in Section 5 can be developed and integrated with one another to develop a master test plan. The prospects of a defect fingerprint that will allow identification and isolation of defects under DC conditions is the final goal.

One of the other big topics of discussion in relation to PD measurements under DC is the method to measure, acquire and process data. Since the test results under DC are most commonly in terms of pulse sequence information, time or a function of time, the characterization of the measurement and acquisition system becomes highly relevant. Dropping or missing a few intermittent pulses over a pulse stream can completely hamper the outcomes of the interpretation of the test data. Therefore, recognizing and defining the limitations of the acquisition systems such as the trigger threshold, sampling rates, bandwidth and sensitivity are essential.

7. Conclusions

Corona is one of the most highly documented and studied defect as

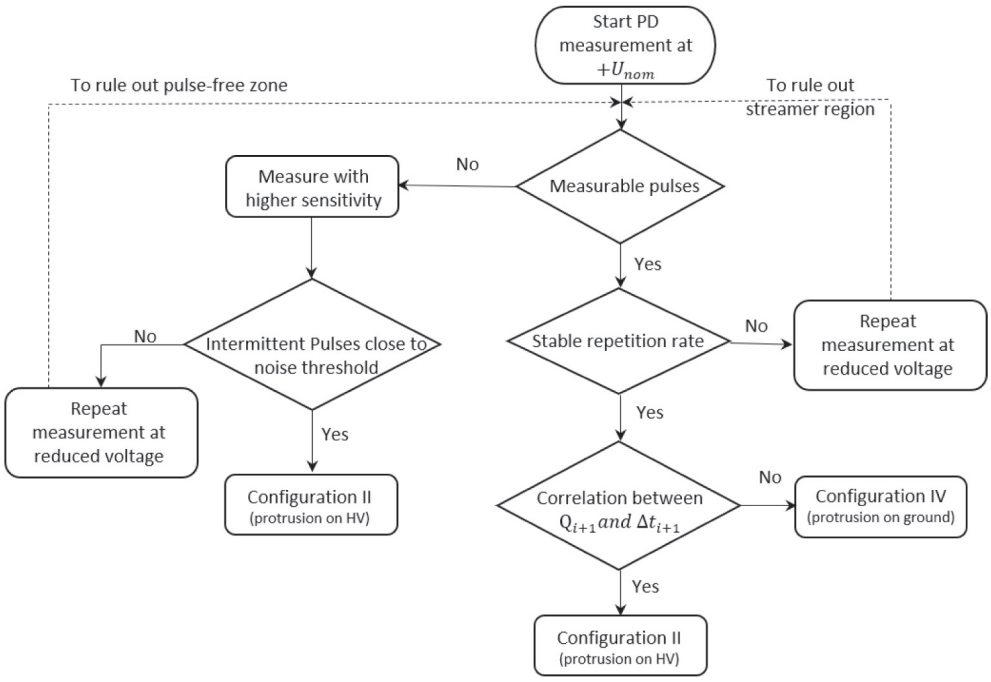

(a) PD test under positive DC voltage.

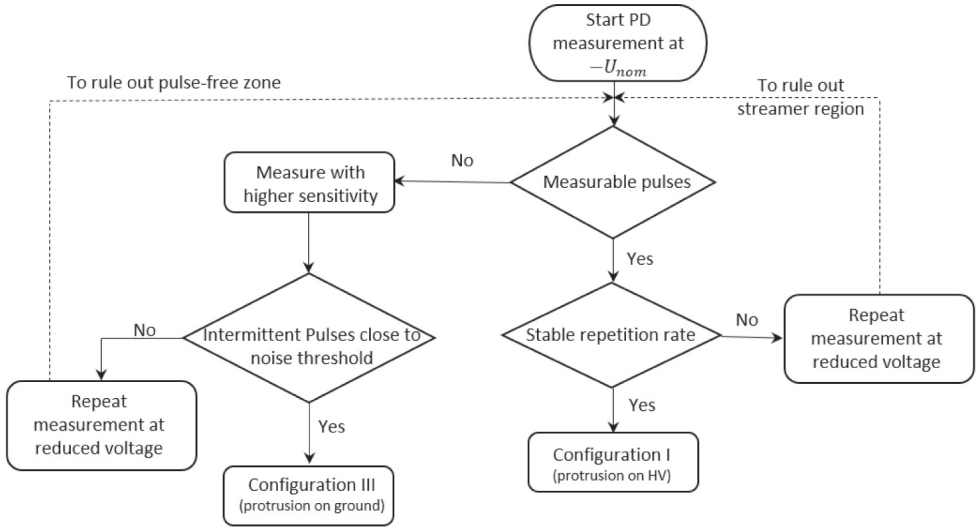

(b) PD test under negative DC voltage.

Fig. 22. Flow chart of the proposed test plan for identifying corona discharge and its configuration under (a) positive DC voltage and (b) negative DC voltage.

it is a part of several beneficial industrial processes such as ozone generation, surface treatments, decontamination of gas streams etc. The integration of available knowledge in diverse fields to further the understanding and interpretation in terms of PD pulse diagrams for corona characterization under High Voltage DC applications is what this paper accomplishes. Several features such as the self-sustaining corona and intermittent corona have been described in journals of applied physics and its applicability towards PD defect identification is exploited through this contribution. The following are the important concluding remarks:

1. There are four instead of two corona configurations based on the position of the protrusion and the polarity of voltage.
2. Each of these four configurations of corona behaves differently from the other. The greatest similarity amongst them is between configuration I and IV. They only differ in terms of discharge inception voltage and discharge magnitude, the defect progression itself remains similar.
3. The plot of the discharge parameter, charge (Q_{i+1}) vs time to discharge (Δt_{i+1}) proves to hold the information towards the mechanism of discharge.
4. In comparison to the PSA plots (ΔQ_i *vs* ΔQ_{i+1}, Δt_i *vs* Δt_{i+1} and ΔQ_i *vs* Δt_i) the plot of charge (Q_{i+1}) vs time to discharge (Δt_{i+1}) is shown to be more robust to outliners and other inherent effects such as double corona source over the protrusion at increased voltages.
5. Minute behavioral features such as the inception of intermittent corona under configuration II and III and the self-sustaining pulse stream of configuration II are pointers for the identification of the origin of the corona (whether from HV terminal or ground).
6. The riskiest configuration of corona is $-$DC applied with protrusion fixed on ground plane (Configuration III). The streamers in this configuration incept at a low voltage level and it subsequently

breaks down at a reduced voltage. This has also been corroborated based on industrial testing experience where most often tests with negative DC voltages have faced problems due to corona coming from improper ground connections.

7. To ascertain the fitness and quality of DC components (currently, with respect to corona defects alone) the component has to be tested at nominal test voltage and its sub-multiples following the test schematic as described in Section 5.

CRediT authorship contribution statement

S. Abdul Madhar: Conceptualization, Methodology, Software, Investigation, Formal analysis, Writing - original draft. **P. Mráz:** Conceptualization, Validation, Resources, Supervision, Project administration, Writing - review & editing. **A. Rodrigo Mor:** Validation, Supervision, Project administration, Writing - review & editing. **R. Ross:** Supervision.

Declaration of Competing Interest

The authors declare that they have no known competing financial interests or personal relationships that could have appeared to influence the work reported in this paper.

Acknowledgment

This work has received funding from the European Union's Horizon 2020 research and innovation programme under the Marie Sklodowska-Curie grant agreement No. 676042.

References

[1] Mraz P, Treyer P, Hammer U. Evaluation and limitations of corona discharge measurements – an application point of view. 2016 International conference on condition monitoring and diagnosis (CMD), Xi'an; 2016. p. 278–81.
[2] Stuckenholz CH, Gamlin M, Mraz P. PD performance of UHV-DC test equipment. Proceedings of the 19th international symposium on high voltage engineering, ISH; 2015.
[3] Kreuger FH. Industrial high DC voltage. Delft University Press; 1995. ISBN 90-407-1110-0.
[4] Chen S, Wang F, Sun Q, Zeng R. Branching characteristics of positive streamers in nitrogen-oxygen gas mixtures. IEEE Trans Dielectr Electr Insul June 2018;25(3):1128–34.
[5] Mraz P, Madhar SA, Treyer P, Hammer U. Guidelines for PD measurements according to IEC 60270. 21st International symposium on high voltage engineering, Budapest, Hungary; 2019 [in Press].
[6] Wagenaars P, Wouters PAAF, van der Wielen PCJM, Steennis EF. Algorithms for arrival time estimation of partial discharge pulses in cable systems. Conference record of the 2008 IEEE international symposium on electrical insulation, Vancouver, BC; 2008. p. 694–7.
[7] Trichel GW. The mechanism of the negative point to plane corona near onset. Phys Rev 1938;54(12):1078.
[8] Crichton BH. Gas discharge physics. IEE Colloquium Adv HV Technol 1996:3–3.
[9] Zhang Y, Xia Q, Jiang Z, Ouyang J. Trichel pulse in various gases and the key factor for its formation. Sci Rep 2017 Aug 31;7(1):10135.
[10] Giao TN, Jordan JB. Modes of corona discharges in air. In: IEEE transactions on power apparatus and systems, vol. PAS-87, no. 5; May 1968. p. 1207–15.
[11] Giao, Trinh N, Jordan JB. Trichel streamers and their transition into the pulseless glow discharge. J Appl Phys 1970;41(10):3991–9.
[12] Chen She, Li Kelin, Nijdam Sander. Transition mechanism of negative DC corona modes in atmospheric air: from Trichel pulses to pulseless glow. Plasma Sources Sci Technol 2018.
[13] Pirker A, Schichler U. Partial discharge measurement at DC voltage—evaluation and characterization by NoDi* pattern. IEEE Trans Dielectr Electr Insul June 2018;25(3):883–91.
[14] Shih J, Chang P, Lawless A, Yamamoto T. Corona discharge processes. IEEE Trans Plasma Sci 1991;19(6):1152–66.
[15] Trichel GW. The mechanism of the positive point-to-plane corona in air at atmospheric pressure. Phys Rev 1939;55(4):382.
[16] Greenwood Allan. The mechanism of the ring discharge in negative point-to-plane corona. J Appl Phys 1952;23(12):1316–9.

Saliha Abdul Madhar was born in Chennai, India, in 1994. She completed her Bachelor's in Electrical and Electronics engineering in 2015. And later received her MSc degree in Electrical Sustainable Energy with a special focus on High Voltage techniques, from the Delft University of Technology, the Netherlands, in 2017. She is currently a Marie-Sklodowska Curie Researcher working with Haefely AG in Basel, Switzerland while pursuing her PhD with the Delft University of Technology. Her PhD focusses on the study of Partial Discharge phenomenon under DC stress. Her research interests include HV Asset monitoring and diagnostics and dielectric phenomenon in HVDC.

Petr Mraz received his PhD degree in Diagnosis of Electrical Devices from the University of West Bohemia in Pilsen, Czech Republic in 2014. His research specifically focused on Partial Discharge Measurement and Evaluation. He currently works at Haefely AG, where he started in 2014 as an Application Engineer but has since become a Product Manager and Development Project Leader primarily responsible for Partial Discharge product line. He is a member of several CIGRE working groups and the IEC 60270 maintenance team.

Armando Rodrigo Mor is an Industrial Engineer from Universitat Politècnica de València, in Valencia, Spain, with a Ph.D. degree from this university in electrical engineering. During many years he has been working at the High Voltage Laboratory and Plasma Arc Laboratory of the Instituto de Tecnología Eléctrica in Valencia, Spain. Since 2013 he is an Assistant Professor in the Electrical Sustainable Energy Department at Delft University of Technology, Delft, The Netherlands. His research interests include monitoring and diagnostic, sensors for high voltage applications, high voltage engineering, and HVDC.

Robert Ross is professor at TU Delft, director of IWO (Institute for Science & Development, Ede), professor at HAN University of Applied Sciences and Asset Management Research Strategist at TenneT (TSO in the Netherlands and part of Germany). At KEMA he worked on reliability and post-failure forensic investigations. His interests concern reliability statistics, electro-technical materials, sustainable technology and superconductivity. For energy inventions he was granted a SenterNovem Annual award and nominated Best Researcher by the World Technology Network. He recently wrote the Wiley/IEEE book "Reliability Analysis for Asset Management of Electric Power Grids" based on experience with utilities and navy.